FUDMA Journal of Sciences (FJS)
ISSN online: 2616-1370
ISSN print: 2645 - 2944
Vol. 8 No. 5, October, 2024, pp 451 - 463
DOI: https://doi.org/10.33003/fjs-2024-0805-2883

FRACTIONAL MATHEMATICAL MODEL FOR THE TRANSMISSION DYNAMICS AND CONTROL OF HEPATITIS C

Jeremiah Amos, David Omale, *William Atokolo, Emmanuel Abah, Benjamin Idoko Omede, Godwin Onuche Acheneje and Bolarinwa Bolaji

Department of Mathematical Sciences, Prince AbubakarAudu University, Anyigba, Nigeria

*Corresponding authors' email: williamsatokolo@gmail.com

ABSTRACT

This study investigates various epidemiological aspects of Hepatitis C infection by employing a fractional-order mathematical model to evaluate the impact of treatment on the transmission dynamics of the disease. The research identifies conditions for the existence and uniqueness of the solution in the fractional-order case and conducts a stability analysis of the endemic equilibrium using the Lyapunov function method. Numerical simulations, performed using the fractional Adams–Bashforth–Moulton technique, demonstrate the effects of model parameters and fractional-order values on the control and spread of Hepatitis C. Further simulations with surface and contour plots reveal that higher contact rates and reduced treatment effectiveness lead to an increased prevalence of Hepatitis C. The study also concludes that optimizing treatment strategies can significantly decrease the disease's prevalence in the population.

Keywords: Hepatitis C, Fractional, Adam-Bashforth-Moulton, Transmission, Control, Strategies

INTRODUCTION

Hepatitis C virus (HCV) remains a global public health concern, primarily transmitted through blood-to-blood contact. It is responsible for chronic liver diseases, leading to cirrhosis, liver cancer, and even death in severe cases. Despite advancements in treatment, particularly with direct-acting antivirals (DAAs), the prevalence of hepatitis C continues to pose challenges due to asymptomatic infections and difficulties in early detection. Globally, an estimated 58 million people live with chronic HCV infection, with approximately 1.5 million new infections occurring annually, according to the World Health Organization (WHO, 2022). The transmission dynamics of HCV are influenced by several factors, including the rate of contact between susceptible and infected individuals, treatment efficacy, and the role of carriers who may not exhibit symptoms but can still transmit the virus.

Mathematical modeling plays a crucial role in understanding the spread of infectious diseases like hepatitis C. These models provide insights into the factors driving the epidemic and help design and evaluate control strategies. Traditional mathematical models have been extensively used to describe the transmission dynamics of HCV; however, they often fail to account for memory effects or long-term dependencies observed in biological processes. To address this, fractional-order models have gained attention in recent years. Fractional calculus, with its non-local properties, offers a more accurate representation of complex biological phenomena, allowing for the incorporation of memory effects and anomalous diffusion in disease transmission (Diethelm, 2021).

Fractional differential equations (FDEs) extend classical integer-order models In this study, we develop a fractional-order mathematical model to describe the transmission dynamics of hepatitis C, incorporating control strategies such as treatment and preventive measures. The model aims to provide a more accurate framework for analyzing the spread of HCV, taking into account the memory effect inherent in fractional calculus. By simulating various intervention scenarios, we aim to offer insights into the most effective strategies for reducing the prevalence of HCV and achieving long-term control of the infection.

This manuscript is organized as follows: Section 2 presents the formulation of the fractional-order model for HCV transmission, Section 3 outlines the numerical methods used to solve the model, Section 4 discusses the results of the simulations under various control strategies, and Section 5 concludes with recommendations for future research and policy implications.

By incorporating fractional derivatives, which are capable of capturing the memory and hereditary properties of biological systems. In the context of HCV, FDEs allow for a more precise understanding of how the virus spreads over time and how individuals' histories of infection and treatment influence disease progression and transmission. The use of fractional-order models provides a significant advantage in developing more realistic and effective control strategies, especially in the face of persistent challenges such as drug resistance, re-infection, and limited healthcare resources (Podlubny, 2022).

In this study, we develop a fractional-order mathematical model to describe the transmission dynamics of hepatitis C, incorporating control strategies such as treatment as preventive measures. The model aims to provide a more accurate framework for analyzing the spread of HCV, taking into account the memory effectinherent in fractional calculus. By simulating various intervention scenarios, we aim to offer insights into the most effective strategies for reducing the prevalence of HCV and achieving long-term control of the infection.

In recent years, fractional calculus has gained considerable interest among researchers due to its effectiveness in describing the dynamic behavior of various physical systems, as noted by Atokolo et al. (2022). Unlike traditional integer-order models that capture only local characteristics, fractional-order models provide a more comprehensive depiction of the entire system. These models are particularly useful for representing systems with memory effects Atokolo et al., (2022). Fractional-order models are not only more realistic but also more practical compared to classical integer-order models. In biological contexts, the Caputo and Riemann-Liouville derivatives are commonly used as singular kernel fractional derivatives. Additionally, there are

non-singular derivatives such as the Mittag-Leffler and Atangana-Baleanu operators.

Atokolo et al. (2022) introduced a fractional-order Sterile Insect Technology (SIT) model to control the spread of the Zika virus, using the LADM to derive solutions as infinite series that converge to the exact value.

In 2024, Atokolo et al. explored various epidemiological aspects of Lassa fever through a fractional-order mathematical model. Their aim was to assess how treatment and vaccination influence the transmission dynamics of Lassa fever, employing a power-law fractional derivative to deepen understanding of the disease's behavior.

Yunus et al. (2022) analyzed the spread and control of COVID-19 in Nigeria using the Caputo fractional-order derivative through LADM, finding that recovery rates at the integer order were higher due to factors like treatment and vaccination.

Omede et al. (2024) developed a fractional-order compartmental model based on the Caputo derivative to describe the dynamics of soil-transmitted helminth infections, producing series solutions via LADM. Their results indicated that the infinite series converged to the exact solution, and the fractional-order model provided more flexibility compared to traditional models.

Ahmed et al. (2022) constructed an ABC-fractional order derivative model for predicting the co-epidemic transmission of HIV and COVID-19.

Omame et al. (2022) studied a fractional-order model for co-infection with hepatitis B virus and COVID-19, utilizing the Atangana-Baleanu derivative. They found that infection prevention is essential for controlling both diseases.

Acheneje et al. (2024) proposed a fractional-order model for the co-infection dynamics of COVID-19 and Monkeypox, using LADM for approximate solutions and fitting real-life data. Their findings indicated that increased treatment capacity would help reduce the burden of these diseases.

Smith et al. (2023) conducted a systematic review on the co-infection dynamics of hepatitis C and COVID-19, summarizing recent studies on mathematical models and identifying common methods, key insights, and research gaps to guide future work.

Atokolo et al. (2023) formulated a mathematical model addressing the spread of vector-borne diseases, incorporating vertical transmission and preventive strategies. They used the theory of the basic reproduction number (R0) to analyze the model's dynamic behavior. Their study demonstrated that a reduction in R0 leads to disease elimination over time, while the disease persists if R0 remains high. The model's disease-free and endemic equilibrium states were shown to be both locally and globally stable. Preventive measures such as Insecticide-Treated Nets (ITN), Indoor Residual Spraying (IRS), and condom use were incorporated alongside treatment interventions. Numerical simulations revealed that the comprehensive use of ITN, IRS, and condoms, in conjunction with treatment, significantly reduced the spread of vector-borne diseases.

Fractional-order models provide numerous advantages, particularly due to their flexibility and ability to capture non-local effects. Unlike classical derivatives, fractional derivatives offer a more accurate approximation of real-world data and greater adaptability. They also account for non-local interactions, a feature often ignored by traditional derivatives. A key advantage of fractional-order models is their ability to incorporate memory effects, something classical models cannot achieve due to the unique properties of fractional operators. This has led many researchers to explore fractional differential equations to address these complexities. A notable example is the work of Ullah et al. (2020), as highlighted by Das et al. (2024), which addresses fuzzy Volterra integral equations with degenerate kernels using a hybrid approach. This method, which merges the Laplace transform with the Adomian Decomposition Method, has drawn considerable attention for advancing the theory of fuzzy analytical dynamic equations.

The study has gained considerable recognition for its important contributions to the development of fuzzy analytical dynamic equation theory. In addition, Ali et al. (2017) explored the existence and stability of a three-point boundary value problem, focusing on various forms of Ulam stability. Their research utilized classical non-linear fractional methods to analyze the problem's stability.

The aims of this paper are to:

i. Establish conditions that guarantee the existence and uniqueness of solutions for the fractional model.
ii. Conduct a stability analysis of the endemic equilibrium point using the Lyapunov function method.
iii. Obtain numerical solutions through the fractional Adams–Bashforth–Moulton method.
iv. Carry out numerical simulations for the model.

Upon reviewing multiple studies related to Hepatitis C mathematical models and transmission dynamics, we found that no prior research has examined the transmission dynamics and control of Hepatitis C using fractional calculus alongside the Adams–Bashforth–Moulton method to perform numerical simulations of the model.

The structure of this paper is as follows: Section 2 outlines the model formulation, Section 3 discusses the model analysis, Section 4 presents the numerical results of the fractional-order model, and Section 5 concludes with final remarks.

Additionally, we introduce some fundamental results and definitions from fractional calculus in this section. The study utilizes both the right and left fractional Caputo derivatives as described by Podlubny et al. (1998) and Bonyah et al. (2020). This paper also emphasizes the applications of fractional calculus in solving real-world problems across fields such as physics, engineering, bio-mathematics, and other scientific disciplines.

Definition 1: Let $f \in \Lambda^{\infty}(R)$ then the left and right Caputo fractional derivative of the function f is given by

$$CD_t^{\gamma} f(t) = \left(t^{0}D_t^{-(m-\gamma)} \left(\frac{d}{dt}\right)^{m} f(t) \right)$$

$$CD_t^{\gamma} f(t) = \frac{1}{\Gamma(m-\gamma)} \int_0^t \left((t-\lambda)^{m-\gamma-1} f^{m}(\lambda) \right) d\lambda \quad (1)$$

The same way

$$CD_t^{\gamma} f(t) = \left(D_T^{-(m-\gamma)} \left(\frac{-d}{dt}\right)^{m} \right) f(t)$$

$${}_T^{C}D_T^{\gamma} f(t) = \frac{(-1)^m}{\Gamma(m-\gamma)} \int_t^T (\lambda - t)^{m-\gamma-1} f^{m}(\lambda) d\lambda$$

Definition 2: The generalized Mittag-Leffler function $E_{\alpha,\beta}(x)$ for $x \in R$ is given by

$$E_{\alpha,\beta}(x) = \sum_{m=0}^{\infty} \frac{x^m}{\Gamma(\alpha m+\beta)}, \alpha, \beta > 0 \quad (2)$$

which can also be represented as

$$E_{\alpha,\beta}(x) = xE_{\alpha,\alpha+\beta(x)} + \frac{1}{\Gamma(\beta)} \quad (3)$$

$$E_{\alpha,\beta}(x) = L\left[t^{\beta-1} E_{\alpha,\beta}(\pm\psi t^{\alpha})\right] = \frac{S^{\alpha-\beta}}{S^{\alpha} \pm \psi} \quad (4)$$

Proposition 1.1.

Let $f \in \Lambda^{\infty}(R) \cap C(R)$and $\alpha \in R, m-1 < \alpha < m$, therefore, the conditions given below holds:

1. ${}_{t_0}^{C}D_t^{\gamma} I^{\gamma} f(t) = f(t)$
2. ${}_{t_0}^{C}D_t^{\gamma} I^{\gamma} f(t) = f(t) - \sum_{k-0}^{m-k} \frac{t^k}{K!} f^{k}(t_0)$

MATERIALS AND METHODS

Model formulation

In developing the Hepatitis C integer-order model, the population is categorized into six distinct groups: susceptible individuals. (S) ,These are individuals who have not contracted the infection, Exposed individuals (E_H)individuals who are not yet infectious; Acute infected populace (I_{AH}) population of individuals who are acute infected; Chronic infected population (I_{CR}) Population of individuals who are chronic infected; Treated population (T_H) Population of individuals on treatment but not yet recovered and (R_H) Recovered population.

Hepatitis C Susceptible Individuals (S) is recruited at the rate of λ . The class reduces by natural death rate μ and also by the fraction of individuals becoming infected after having contacts with acute infected individuals, chronic infected individuals and individuals on hepatitis C treatment at rates of ψ_1, ψ_2, ψ_3correspondingly. This Hepatitis C susceptible individuals grow by the rate at which recovered individuals becomes susceptible again at the rate θ. We consequently formulated the dynamics of susceptible individuals as;

$$\frac{dS}{dt} = \lambda + \theta R_H - \left(\frac{(\psi_1 I_{AH} + \psi_2 I_{CR} + \psi_3 T_H)}{N_H}\right) S - \mu S.$$

Hepatitis C Exposed Individuals (E_H) increases as a result of the proportion of individuals that are infected newly at rates of ψ_1, ψ_2, ψ_3 respectively. This group reduces by the rate at which the exposed becomes fully acute infected at the rateρ and by natural death rate μ . This population is formulated as follows;

$$\frac{dE_H}{dt} = \left(\frac{(\psi_1 I_{AH} + \psi_2 I_{CR} + \psi_3 T_H)}{N_H}\right) S - (\rho + \mu) E_H.$$

Hepatitis C acute Infected Individuals (I_{AH})grow due to the progression of the exposed to the infected class at rateρ. The population reduces by natural death rate μ , disease induced death at rate δ_1 , the rate at which the acute infected individuals are taken for treatment at rate α_1 the natural recovery rate φ_1 . Progression rate from acute to chronic stagesσ.The dynamics of this group is formulated as;

$$\frac{dI_{AH}}{dt} = \rho E_H - (\alpha_1 + \phi_1 + \sigma + \delta_1 + \mu) I_{AH}$$

Hepatitis C chronic Infected Individuals (I_{CR}) grows due to the progression of the acute infected individuals to the infected class at rateσ. The population reduces by natural death rate μ , disease induced death at rate δ_2 , the rate at which the chronic infected individuals are taken for treatment at rate α_2 the natural recovery rate φ_2 . The dynamics of this class is formulated as;

$$\frac{dI_{CR}}{dt} = \sigma I_{AH} - (\alpha_2 + \varphi_2 + \delta_2 + \mu) I_{CR}.$$

Hepatitis C infected but on treatment individuals (T_H) increases by the rate at which the infected acute individuals and infected chronic individuals are taken for treatment at rate α_1 and α_2 the population reduces , due to both disease induced and natural death at rate μ and δ_3 respectively. The class finally reduces due to natural recovery natural recovery rateφ_3. The dynamics of this population is hereby presented as;

$$\frac{dT_H}{dt} = \alpha_1 I_{AH} + \alpha_2 I_{CR} - (\varphi_3 + \delta_3 + \mu) T_H.$$

Hepatitis C recovered population(R_H) grows due to rate at which the acute infected individuals, chronic infected individuals and individuals on hepatitis C treatment recovered at the rate of $\varphi_1, \varphi_2, \varphi_3$, the rate at which the recovered individuals become susceptible again to the disease θ. The class finally reduces due to natural death at rate μ . The dynamics of this class is formulated as;

$$\frac{dR_H}{dt} = \varphi_1 I_{AH} + \varphi_2 I_{CR} + \varphi_3 T_H - (\theta + \mu) R_H.$$

The force of infection associated to the population is $\omega_H = \frac{(\psi_1 I_{AH} + \psi_2 I_{CR} + \psi_3 T_H)}{N_H}$,

The model flow diagram corresponding to our assumption is shown in

Fig. 1; In the same way, the mathematical model that corresponds to our assumptions and description above is given by:

$$\begin{aligned}
\frac{dS}{dt} &= \lambda + \theta R_H - \left(\frac{(\psi_1 I_{AH} + \psi_2 I_{CR} + \psi_3 T_H)}{N_H}\right) S - \mu S, \\
\frac{dE_H}{dt} &= \left(\frac{(\psi_1 I_{AH} + \psi_2 I_{CR} + \psi_3 T_H)}{N_H}\right) S - (\rho + \mu) E_H, \\
\frac{dI_{AH}}{dt} &= \rho E_H - (\alpha_1 + \varphi_1 + \sigma + \delta_1 + \mu) I_{AH}, \qquad (5) \\
\frac{dI_{CR}}{dt} &= \sigma I_{AH} - (\alpha_2 + \varphi_2 + \delta_2 + \mu) I_{CR}, \\
\frac{dT_H}{dt} &= \alpha_1 I_{AH} + \alpha_2 I_{CR} - (\varphi_3 + \delta_3 + \mu) T_H, \\
\frac{dR_H}{dt} &= \varphi_1 I_{AH} + \varphi_2 I_{CR} + \varphi_3 T_H - (\theta + \mu) R_H.
\end{aligned}$$

Where $\omega_H = \frac{(\psi_1 I_{AH} + \psi_2 I_{CR} + \psi_3 T_H)}{N_H}$.

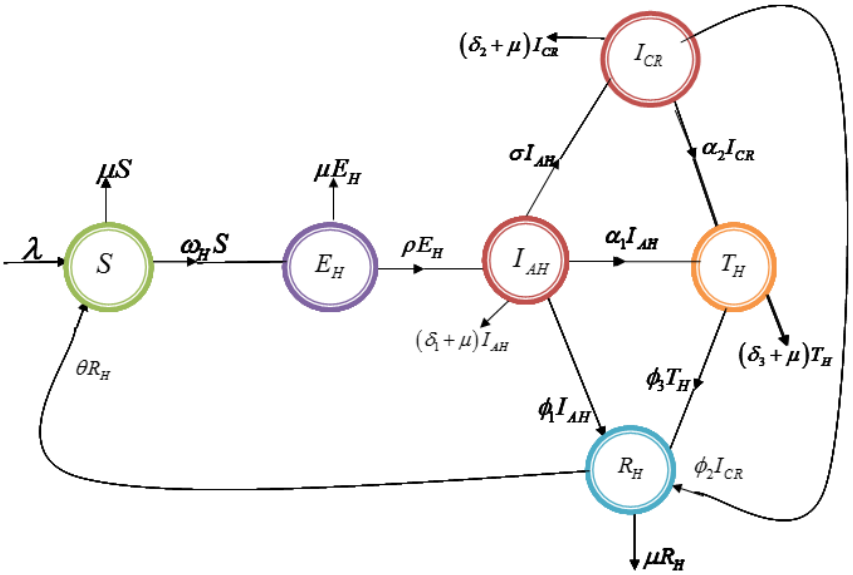

Fractional Hepatitis C mathematical model

In this section, we expand upon the integer-order Hepatitis C model from Eq. (5) by incorporating the Caputo fractional derivative operator. This new model, utilizing the Caputo fractional derivative, offers greater flexibility compared to the classical model in Eq. (5), as the fractional-order model allows for varied responses. The fractional-order Hepatitis C model is thus introduced as follows:

$$CD_t^{\gamma}S = \lambda + \theta R_H - \omega_H S - \mu S,$$
$$CD_t^{\gamma}E_H = \omega_H S - K_1 E_H,$$
$$CD_t^{\gamma}I_{AH} = \rho E_H - K_2 = I_{AH},$$
$$CD_t^{\gamma}I_{CR} = \sigma I_{AH} - K_3 I_{CR},$$
$$CD_t^{\gamma}T_H = \alpha_1 I_{AH} + \alpha_2 I_{CR} - K_4 T_H,$$
$$CD_t^{\gamma}R_H = \varphi_1 I_{AH} + \varphi_2 I_{CR} + \varphi_3 T_H - K_5 R_H.$$

Where $K_1 = (\rho+\mu)$, $K_2 = (\alpha_1+\varphi_1+\sigma+\delta_1+\mu)$, $K_3 = (\alpha_2+\varphi_2+\delta_2+\mu)$, $K_4 = (\varphi_3+\delta_3+\mu)$, $K_5 = (\theta+\mu)$. (7)

Subject to the positive initial conditions

$$S(0) = S_0, E_H(0) = E_{H0}, I_{AH}(0) = I_{AH0}, I_{CR}(0) = I_{CR0}, T_H(0) = T_{H0}, R_H(0) = R_{H0}.(8).$$

Positivity of model solution

We considered the non-negativity of the initial values

$$lim\, S\, up N_H(t) \leq \frac{\lambda}{\mu},$$

Secondly, If $lim\, S\, up N_{H0}(t) \leq \frac{\lambda}{\mu}$, then our model feasible domain is given by:

$$\Omega = \left\{(S, E_H, I_{AH}, I_{CR}, T_H, R_H) \subset R_+^6 : S + E_H + I_{AH} + I_{CR} + T_H + R_H \leq \frac{\lambda}{\mu}\right\},$$ so that

$$\Omega = \Omega_H \subset R_+^6,$$

hence, Ω is positively invariant.

If $S_0, E_{H0}, I_{AH0}, I_{CR0}, T_{H0}, R_{H0}$ are non-negative, then the solution of model (6) will be non-negative for $t > 0$. From Eq. (6), picking the first equation, we have that

$$CD_t^{\gamma}S = \lambda + \theta R_H - \omega_H S - \mu S,$$
$$CD_t^{\gamma}S = \lambda + \theta R_H - (\omega_H + \mu)S,$$
$$CD_t^{\gamma}S + (\omega_H + \mu)S = \lambda + \theta R_H,$$

But $\lambda + \theta R_H \geq 0$,then,

$$CD_t^{\gamma}S + (\omega_H + \mu)S \geq 0,$$

Applying the Laplace transform we obtained;

$$L\left[CD_t^{\gamma}S\right] + L[(\omega_H + \mu)S] \geq 0,$$
$$S^{\gamma}S(s) - S^{\gamma-1}S(0) + (\omega_H + \mu)S(s) \geq 0,$$
$$S(s) \geq \frac{S^{\gamma-1}}{S^{\gamma} + (\omega_H + \mu)}S(0),$$

By taking the inverse Laplace transform, we obtained ;

$$S(t) \geq E_{\gamma,1}(-(\omega_H + \mu)t^{\gamma})S_0, \quad (9)$$

Now since the term on the right hand side of Eq. (9) is positive, we conclude that for$t > 0$. In similar way, we say that$S \geq 0, E_H \geq 0, I_{AH} \geq 0, I_{CR} \geq 0, T_H \geq 0, R_H \geq 0$. that is are positives, consequently, the solution will remain in R_+^6 for all $t > 0$ with positive initial situation.

Boundedness of fractional model solution

The total population of individuals from our model is given by ;

$$N_H(t) = S(t) + E_H(t) + I_{AH}(t) + I_{CR}(t) + T_H(t) + R_H(t).$$

So from our fractional model (6), we now obtain

$$CD_t^{\gamma}N_H(t) = {}^{C}D_t^{\gamma}S(t) + {}^{C}D_t^{\gamma}E_H(t) + {}^{C}D_t^{\gamma}I_{AH}(t) + {}^{C}D_t^{\gamma}I_{CR}(t) + {}^{C}D_t^{\gamma}T_H(t) + {}^{C}D_t^{\gamma}R_H(t)$$
$$CD_t^{\gamma}N_H(t) \leq \lambda - \mu N_H(t) \quad (10)$$

Taking the Laplace transformation of (10) we now have;

$$L\left[CD_t^{\gamma}N_H(t)\right] \leq L[\lambda - \mu N_H(t)],$$
$$S^{\gamma}N_H(s) - S^{\gamma-1}N_H(0) + \mu N_H(s) \leq \frac{\lambda}{\mu},$$
$$N_H(s) \leq \frac{S^{\gamma-1}}{(S^{\gamma}+\mu)}N_H(0) + \frac{\lambda}{S(S^{\gamma}+\mu)}, \quad (11)$$

Taking the inverse Laplace transform of Eq. (11) we have ;

$$N_H(t) \leq E_{\gamma,1}(-\mu t^{\gamma})N_H(0) + \lambda E_{\gamma,\gamma+1}(-\mu t^{\gamma}), \quad (12)$$

At$t \to \infty$,, the limit of Eq. (12) becomes;

$$\lim_{t\to\infty} Sup N_H(t) = \frac{\lambda}{\mu}.$$

This means that, if $N_{H0} \leq \frac{\lambda}{\mu}$ then $N_H \leq \frac{\lambda}{\mu}$ which implies that,$N_H(t)$ is enclosed or bounded.

We now conclude that, this region$\Omega = \Omega_H$, is well posed and similarly feasible epidemiologically.

Existence and uniqueness of our model solution

Let the real non-negative be P, we $Q = [0, P]$.

The set of all continuous function that is defined on M is represented by $N_e^0(Q)$ with norm as;

$$\|X\| = Sup\{|X(t)|, t \in Q\}.$$

Considering model (6) with initial conditions presented in (8) which can be denoted as an initial value problem (IVP) in (13).

$cD_t^{\gamma}(t) = Z\big(t, X(t)\big), 0 < t < P < \infty,$
$X(0) = X_0.$
Where $Y(t) = \big(S(t), E_H(t), I_{AH}(t), I_{CR}(t), T_H(t), R_H(t)\big)$ represents the groups and Z be a continuous function defined as follows;

$$= \begin{pmatrix} \lambda + \theta R_H - \left(\frac{(\psi_1 I_{AH} + \psi_2 I_{CR} + \psi_3 T_H)}{N_H}\right) S - \mu S \\ \left(\frac{(\psi_1 I_{AH} + \psi_2 I_{CR} + \psi_3 T_H)}{N_H}\right) S - (\rho + \mu) E_H \\ \rho E_H - (\alpha_1 + \varphi_1 + \sigma + \delta_1 + \mu) I_{AH} \\ \sigma I_{AH} - (\alpha_2 + \varphi_2 + \delta_2 + \mu) I_{CR} \\ \alpha_1 I_{AH} + \alpha_2 I_{CR} - (\varphi_3 + \delta_3 + \mu) T_H \\ \varphi_1 I_{AH} + \varphi_2 I_{CR} + \varphi_3 T_H - (\theta + \mu) R_H \end{pmatrix} \quad (14)$$

Using proposition (2.1), we have that,

$$S(t) = S_0 + I_t^{\gamma}\left[\lambda + \theta R_H - \left(\frac{(\psi_1 I_{AH} + \psi_2 I_{CR} + \psi_3 T_H)}{N_H}\right) S - \mu S\right],$$
$$E_H(t) = E_{H0} + I_t^{\gamma}\left[\left(\frac{(\psi_1 I_{AH} + \psi_2 I_{CR} + \psi_3 T_H)}{N_H}\right) S - (\rho + \mu) E_H\right], \quad (15)$$
$$I_{AH}(t) = I_{AH0} + I_t^{\gamma}[\rho E_H - (\alpha_1 + \varphi_1 + \sigma + \delta_1 + \mu) I_{AH}],$$
$$I_{CR}(t) = I_{CR0} + I_t^{\gamma}[\sigma I_{AH} - (\alpha_2 + \varphi_2 + \delta_2 + \mu) I_{CR}],$$
$$T_H(t) = T_{H_0} + I_t^{\gamma}[\alpha_1 I_{AH} + \alpha_2 I_{CR} - (\varphi_3 + \delta_3 + \mu) T_H],$$
$$R_H(t) = R_{H_0} + I_t^{\gamma}[\varphi_1 I_{AH} + \varphi_2 I_{CR} + \varphi_3 T_H - (\theta + \mu) R_H].$$

We have the Picard iteration of (15) as follows;

$$S(t) = S_0 + \frac{1}{\Gamma(\gamma)}\int_0^t (t-\lambda)^{\gamma-1} Z_1\big(\lambda, S_{n-1}(\lambda)\big) d\lambda, \quad (16)$$
$$E_H(t) = E_{H_0} + \frac{1}{\Gamma(\gamma)}\int_0^t (t-\lambda)^{\gamma-1} Z_2\left(\lambda, E_{H_{(n-1)}}(\lambda)\right) d\lambda,$$
$$I_{AH}(t) = I_{AH_0} + \frac{1}{\Gamma(\gamma)}\int_0^t (t-\lambda)^{\gamma-1} Z_3\left(\lambda, I_{AH_{(n-1)}}(\lambda)\right) d\lambda,$$
$$I_{CR}(t) = I_{CR_0} + \frac{1}{\Gamma(\gamma)}\int_0^t (t-\lambda)^{\gamma-1} Z_4\left(\lambda, I_{CR_{(n-1)}}(\lambda)\right) d\lambda,$$
$$T_H(t) = T_{H_0} + \frac{1}{\Gamma(\gamma)}\int_0^t (t-\lambda)^{\gamma-1} Z_5\left(\lambda, T_{H_{(n-1)}}(\lambda)\right) d\lambda,$$
$$R_H(t) = R_{H_0} + \frac{1}{\Gamma(\gamma)}\int_0^t (t-\lambda)^{\gamma-1} Z_6\left(\lambda, R_{H_{(n-1)}}(\lambda)\right) d\lambda.$$

We now transformed the initial value problem of Eq. (13) to obtain ;

$$X(t) = X(0) + \frac{1}{\Gamma(\gamma)}\int_0^t (t-\lambda)^{\gamma-1} Z\big(\lambda, X(\lambda)\big) d\lambda. \quad (17)$$

Lemma 1, The Lipchitz condition described from Eq. (14) is satisfied by vector $Z\big(t, X(\lambda)\big)$ on a set $[0, P] \times R_+^6$ with the Lipchitz constant given as;

$$\beta = max\big((\psi_1^* + \psi_2^* + \psi_3^* + \mu), (\rho + \mu), (\alpha_1 + \varphi_1 + \sigma + \delta_1 + \mu), (\alpha_2 + \varphi_2 + \delta_2 + \mu), (\varphi_3 + \delta_3 + \mu)\big).$$

Proof.

$$\|Z_1(t, S) - Z_1(t, S_1)\| = \left\|\lambda + \theta R_H - \left(\frac{(\psi_1 I_{AH} + \psi_2 I_{CR} + \psi_3 T_H) + \mu}{N_H}\right) S - \lambda - \theta R_H - \left(\frac{(\psi_1 I_{AH} + \psi_2 I_{CR} + \psi_3 T_H) + \mu}{N_H}\right) S_1\right\|$$
$$= \left\|-\left(\frac{(\psi_1 I_{AH} + \psi_2 I_{CR} + \psi_3 T_H) + \mu}{N_H}\right)(S - S_1) + \mu(S - S_1)\right\|$$
$$\leq -\big((\psi_1^* + \psi_2^* + \psi_2^*)\big)\|(S - S_1)\| + \|\mu(S - S_1)\|$$
$$\therefore \|Z_1(t, S) - Z_1(t, S_1)\| \leq \big((\psi_1^* + \psi_2^* + \psi_2^* + \mu)\big)\|(S - S_1)\| + \|\mu(S - S_1)\|$$

Similarly we obtained the following;

$$\|Z_2(t, E_H) - Z_2(t, E_{H1})\| \leq (\rho + \mu)\big\|(E_H - E_{H_1})\big\|,$$
$$\|Z_3(t, I_{AH}) - Z_3(t, I_{AH1})\| \leq (\alpha_1 + \varphi_1 + \sigma + \delta_1 + \mu)\big\|(I_{AH} - I_{AH_1})\big\|, \quad (18)$$
$$\|Z_4(t, I_{CR}) - Z_4(t, I_{CR1})\| \leq (\alpha_2 + \varphi_2 + \delta_2 + \mu)\big\|(I_{CR} - I_{CR_1})\big\|,$$
$$\|Z_5(t, T_H) - Z_5(t, T_{H1})\| \leq (\varphi_3 + \delta_3 + \mu)\big\|(T_H - T_{H_1})\big\|,$$
$$\|Z_6(t, R_H) - Z_6(t, R_{H1})\| \leq (\theta + \mu)\big\|(R_H - R_{H_1})\big\|.$$

Where we obtained

$$\big\|Z_1\big(t, X_1(t)\big) - Z\big(t, X_2(t)\big)\big\| \leq \beta\|X_1 - X_2\|,$$
$$\beta = max\big((\psi_1^* + \psi_2^* + \psi_3^* + \mu), (\rho + \mu), (\alpha_1 + \varphi_1 + \sigma + \delta_1 + \mu), (\alpha_2 + \varphi_2 + \delta_2 + \mu), (\varphi_3 + \delta_3 + \mu)\big). \quad (19)$$

Lemma 2. The initial value problem (6), (7) in Eq. (19) exists and will have a unique solution
$X(t) \in A_c^0(f).$
Using Picard-Lindelof and fixed point theory, we estimate the solution of
$X(t) = S\big(X(t)\big),$
where S is defined as the Picard operator articulated as ;
$S: A_c^0(f, R_+^6) \to A_c^0(f, R_+^6)$
Therefore

$$S\big(X(t)\big) = X(0) + \frac{1}{\Gamma(\gamma)}\int_0^t (t-\lambda)^{\gamma-1} Z_1\big(\lambda, X(\lambda)\big) d\lambda,$$

which becomes $\big\|S\big(X_1(t)\big) - S(X_2(t))\big\|$

$$= \frac{1}{\Gamma(\gamma)}\left[\int_0^t (t-\lambda)^{\gamma-1} Z\big(\lambda, X_1(\lambda)\big) - Z\big(\lambda, X_2(\lambda)\big) d\lambda\right],$$
$$\leq \frac{1}{\Gamma(\gamma)}\left[\int_0^t (t-\lambda)^{\gamma-1} Z\big(\lambda, X_1(\lambda)\big) - Z\big(\lambda, X_2(\lambda)\big) d\lambda\right],$$
$$\leq \frac{\beta}{\Gamma(\gamma)}\left[\int_0^t (t-\lambda)^{\gamma-1} \|X_1 - X_2\| d\lambda\right],$$
$$\big\|S\big(X_1(t) - SX_2(t)\big)\big\| \leq \frac{\beta}{\Gamma(\gamma+1)S}.$$

When, $\frac{\beta}{\Gamma(\gamma+1)} S \leq 1$. then the Picard operator gives a negation , so Eq.(6) , (7) solution is unique.

The basic reproduction number (R_0) and model equilibrium points

The disease free equilibrium point of the model (5) is expressed as:

$$(HDFEP) = (S^*, E_H^*, I_{AH}^*, I_{CR}^*, T_H^*, R_H^*) = \left(\frac{\lambda}{\mu}, 0, 0, 0, 0, 0\right) \quad (20)$$

In calculating the basic reproduction number, we consider the method used in [22].

Let $n = \big(E_H, I_{AH}, I_{CR}, T_H\big)$
So that, $\frac{dn}{dt} = F - V$
Where,

$$F = \begin{bmatrix} 0 & \psi_1 & \psi_2 & \psi_3 \\ 0 & 0 & 0 & 0 \\ 0 & 0 & 0 & 0 \\ 0 & 0 & 0 & 0 \end{bmatrix}$$
$$V = \begin{bmatrix} K_1 & 0 & 0 & 0 \\ -\rho & K_2 & 0 & 0 \\ 0 & -\sigma & K_3 & 0 \\ 0 & -\alpha_1 & -\alpha_2 & K_4 \end{bmatrix},$$

Let, , , $K_1 = (\rho + \mu), K_2 = (\alpha_1 + \varphi_1 + \sigma + \delta_1 + \mu), K_3 = (\alpha_2 + \varphi_2 + \delta_2 + \mu), K_4 = (\varphi_3 + \delta_3 + \mu).$

Mathematically, the basic reproduction number is calculated as $R_0^H = \rho(FV^{-1})$ where ρ is the leading Eigen value of the systemFV^{-1}. Where R_0^H is the basic reproduction number associated with the individuals in the population.

$$R_0^H = \frac{\rho(\sigma K_4\psi_2 + \sigma\alpha_2 K_4\psi_3 + K_3K_4\psi_1 + \alpha_1 K_3\psi_3)}{K_1K_2K_3K_4}$$

Since $K_1 = (\rho+\mu), K_2 = (\alpha_1+\varphi_1+\sigma+\delta_1+\mu), K_3 = (\alpha_2+\varphi_2+\delta_2+\mu), K_4 = (\varphi_3+\delta_3+\mu)$.

$$R_0^H = \frac{\rho(\sigma K_4(\varphi_3+\delta_3+\mu)\psi_2+\sigma\alpha_2K_4(\varphi_3+\delta_3+\mu)\psi_3+(\alpha_2+\varphi_2+\delta_2+\mu)(\varphi_3+\delta_3+\mu)\psi_1+\alpha_1K_3\psi_3)}{(\rho+\mu)(\alpha_1+\varphi_1+\sigma+\delta_1+\mu)(\alpha_2+\varphi_2+\delta_2+\mu)(\varphi_3+\delta_3+\mu)} \quad (21)$$

Endemic equilibrium point

We investigated the potential for the existence of an endemic equilibrium point, which represents a stable state where Hepatitis C remains present within the population. At this equilibrium, the model's variables maintain positive, non-zero values.
$(S^* \neq 0, E_H^* \neq 0, I_{AH}^* \neq 0, I_{CR}^* \neq 0, T_H^* \neq 0, R_H^* \neq 0)$..

To examine the endemic equilibrium point, the model equations are expressed in relation to the infection rates in the populations. From the fractional Hepatitis C model (6), the endemic equilibrium state is represented by:
$E_{**} = (S^{**}, E_H^{**}, I_{AH}^{**}, I_{CR}^{**}, T_H^{**}, R_H^{**})$,
defined as;

$$S^{**} = \frac{A_2A_3A_4A_5A_6\lambda}{A_1A_2A_3A_4A_5A_6 - \omega_H^{**}A_5\rho\theta(A_4\varphi_1+\sigma\varphi_2) - \omega_H^{**}\varphi_3\rho\theta(A_4A_5\alpha_1+\sigma\alpha_2)},$$

$$E_H^{**} = \frac{\omega_H^{**}A_3A_4A_5A_6\lambda}{A_1A_2A_3A_4A_5A_6 - \omega_H^{**}A_5\rho\theta(A_4\varphi_1+\sigma\varphi_2) - \omega_H^{**}\varphi_3\rho\theta(A_4A_5\alpha_1+\sigma\alpha_2)},$$

$$I_{AH}^{**} = \frac{\omega_H^{**}\rho A_4A_5A_6\lambda}{A_1A_2A_3A_4A_5A_6 - \omega_H^{**}A_5\rho\theta(A_4\varphi_1+\sigma\varphi_2) - \omega_H^{**}\varphi_3\rho\theta(A_4A_5\alpha_1+\sigma\alpha_2)},$$

$$I_{CR}^{**} = \frac{\omega_H^{**}\rho\sigma A_5A_6\lambda}{A_1A_2A_3A_4A_5A_6 - \omega_H^{**}A_5\rho\theta(A_4\varphi_1+\sigma\varphi_2) - \omega_H^{**}\varphi_3\rho\theta(A_4A_5\alpha_1+\sigma\alpha_2)}, \quad (22)$$

$$T_H^{**} = \frac{\omega_H^{**}A_6\lambda(\rho\alpha_1+\sigma\rho\alpha_2)}{A_1A_2A_3A_4A_5A_6 - \omega_H^{**}A_5\rho\theta(A_4\varphi_1+\sigma\varphi_2) - \omega_H^{**}\varphi_3\rho\theta(A_4A_5\alpha_1+\sigma\alpha_2)},$$

$$R_H^{**} = \frac{\omega_H^{**}\rho A_5\lambda(A_4\varphi_1+\sigma\varphi_2) + \varphi_3\omega_H^{**}\rho\lambda(A_4A_5\alpha_1+\sigma\alpha_2)}{A_1A_2A_3A_4A_5A_6 - \omega_H^{**}A_5\rho\theta(A_4\varphi_1+\sigma\varphi_2) - \omega_H^{**}\varphi_3\rho\theta(A_4A_5\alpha_1+\sigma\alpha_2)}.$$

Where $A_1 = (\rho+\mu)$, $A_2 = (\alpha_1+\varphi_1+\sigma+\delta_1+\mu)$, $A_3 = (\alpha_2+\varphi_2+\delta_2+\mu)$,$A_4 = (\varphi_3+\delta_3+\mu)$,$A_5 = (\theta+\mu)$.
But Substituting the equations above into the force of infection we have;
$f(\omega_H^{**}) = \omega_H^{**}B_1 + B_2 = 0$
Where

$$B_1 = \left(A_3A_4A_5A_6\lambda + \rho A_4A_5A_6\lambda + \rho\sigma A_5A_6\lambda + A_6\lambda(\alpha_1\rho+\alpha_2\rho\sigma) + \rho\lambda A_5(\varphi_1A_4+\varphi_2\sigma) + \varphi_3\rho\lambda(\alpha_1A_4A_5+\alpha_2\sigma)\right)$$

$$B_2 = A_2A_3A_4A_5A_6\lambda\left(1 - \frac{\rho(\sigma A_5\psi_2 + \sigma\alpha_2A_5\psi_3 + A_4A_5\psi_1 + \alpha_1A_4\psi_3)}{A_2A_3A_4A_5}\right)$$

$$B_2 = A_2A_3A_4A_5A_6\lambda(1-R_0) \quad (23)$$

Which imply that , the model (6) above have a stable endemic equilibrium point.

Global stability analysis at endemic equilibrium state

The global stability of the equilibrium point is analyzed using the direct Lyapunov method. The endemic equilibrium point is globally stable when $(R_0 > 1)$, which shows that the disease will increasein the population irrespective of the initial conditions. This is derived from the fractional model (6).

$$\omega_H = \frac{\psi_1 I_{AH}}{N_H} + \frac{\psi_2 I_{CR}}{N_H} + \frac{\psi_3 T_H}{N_H}$$

Where$N_H \leq \frac{\lambda}{\mu}$ a s $t \to \infty$**,**
then$\omega_H = \psi_1 I_{AH} + \psi_2 I_{CR} + \psi_3 T_H$
our fractional model now becomes

$$\begin{aligned}
&CD_t^\gamma S = \lambda + \theta R_H - \omega_H S - \mu S,\\
&CD_t^\gamma E_H = \omega_H S - K_1 E_H,\\
&CD_t^\gamma I_{AH} = \rho E_H - K_2 = I_{AH},\\
&CD_t^\gamma I_{CR} = \sigma I_{AH} - K_3 I_{CR},\\
&CD_t^\gamma T_H = \alpha_1 I_{AH} + \alpha_2 I_{CR} - K_4 T_H,\\
&CD_t^\gamma R_H = \varphi_1 I_{AH} + \varphi_2 I_{CR} + \varphi_3 T_H - K_5 R_H.
\end{aligned} \quad (24)$$

Where $K_1 = (\rho+\mu)$, $K_2 = (\alpha_1+\varphi_1+\sigma+\delta_1+\mu)$, $K_3 = (\alpha_2+\varphi_2+\delta_2+\mu)$,$K_4 = (\varphi_3+\delta_3+\mu)$,$K_5 = (\theta+\mu)$.

At equilibrium point Eq. (24) has the following results
$\lambda = \omega_{H1}^{**}S^{**} + \mu S^{**} - \theta R_H^{**}$, $K_1E_H^{**} = \omega_H^{**}S^{**}$, $K_2I_{AH}^{**} = \rho E_H^{**}$, $K_4T_H^{**} = \alpha_1I_{AH}^{**} + \alpha_2I_{CR}^{**}$, $K_5R_H^{**} = \varphi_1I_{AH}^{**} + \varphi_2I_{CR}^{**} + \varphi_3T_H^{**}$.

Theorem 1.
Model (24) is globally asymptotically stable if $R_0^H > 1$
whenever

$$\left(6 - \frac{S^{**}}{S} + \frac{\omega_{H1}}{\omega_{H1}^{**}}\left(1 - \frac{SE_H^{**}}{S^{**}E_H}\right) - \frac{I_{AH}^{**}E_H}{I_{AH}E_H^{**}} - \frac{I_{CR}^{**}I_{AH}}{I_{CR}I_{AH}^{**}} - \frac{T_H}{T_H^{**}} - \frac{T_H^{**}I_{AH}I_{CR}}{T_HI_{AH}^{**}I_{CR}^{**}}\right) \leq 0.$$

$$L(t) = L_H(t)$$

be a non-linear Lyaponov function as presented in (25) below:

$$L(t) = L_1\left(S - S^{**} - S^{**}\,ln\frac{S}{S^{**}}\right) + L_2\left(E_H - E_H^{**} - E_H^{**}\,ln\frac{E_H}{E_H^{**}}\right) + L_2\left(E_H - E_H^{**} - E_H^{**}\,ln\frac{E_H}{E_H^{**}}\right)$$
$$+L_3\left(I_{AH} - I_{AH}^{**} - I_{AH}^{**}\,ln\frac{I_{AH}}{I_{AH}^{**}}\right) + L_4\left(I_{CR} - I_{CR}^{**} - I_{CR}^{**}\,ln\frac{I_{CR}}{I_{CR}^{**}}\right) + L_5\left(T_H - T_H^{**} - T_H^{**}\,ln\frac{T_H}{T_H^{**}}\right)$$
$$+L_6\left(R_H - R_H^{**} - R_H^{**}\,ln\frac{R_H}{R_H^{**}}\right). \quad (25)$$

Taking the Caputo Fractional order derivative of Eq. (25), we have

$${}^cD_t^\gamma L(t) = {}^cD_t^\gamma L_H(t) \leq L_1\left(1 - \frac{S^{**}}{S}\right){}^cD_t^\gamma S(t) + L_2\left(1 - \frac{E_H^{**}}{E_H^{**}}\right){}^cD_t^\gamma E_H(t) + L_3\left(1 - \frac{I_{AH}^{**}}{I_{AH}^{**}}\right){}^cD_t^\gamma I_{AH}(t)$$
$$+L_4\left(1 - \frac{I_{CR}^{**}}{I_{CR}^{**}}\right){}^cD_t^\gamma I_{CR}(t) + L_5\left(1 - \frac{T_H^{**}}{T_H^{**}}\right){}^cD_t^\gamma T_H(t) + L_6\left(1 - \frac{R_H^{**}}{R_H^{**}}\right){}^cD_t^\gamma R_H(t), =$$
$$\omega_{H1}^{**}S^{**}\left(\begin{matrix}\left(1 - \frac{S^{**}}{S}\right){}^cD_t^\gamma S(t) + \left(1 - \frac{E_H^{**}}{E_H}\right){}^cD_t^\gamma E_H(t) + \left(1 - \frac{I_{AH}^{**}}{I_{AH}}\right){}^cD_t^\gamma I_{AH}(t) \\ \left(1 - \frac{I_{CR}^{**}}{I_{CR}}\right){}^cD_t^\gamma I_{CR}(t) + \left(1 - \frac{T_H^{**}}{T_H}\right){}^cD_t^\gamma T_H(t) + \left(1 - \frac{R_H^{**}}{R_H}\right){}^cD_t^\gamma R_H(t)\end{matrix}\right).$$

$$\left(1 - \frac{S^{**}}{S}\right){}^cD_t^\gamma S = \left(1 - \frac{S^{**}}{S}\right)(\omega_{H1}^{**}S^{**} + \mu S^{**} - \theta R_H - \omega_{H1}S - \mu S + \theta R_H),$$
$$= \omega_{H1}^{**}S^{**}\left(\left(1 - \frac{S\omega_{H1}}{\omega_{H1}^{**}S^{**}} - \frac{S^{**}}{S} + \frac{\omega_{H1}}{\omega_{H1}^{**}}\right) + \mu S^{**}\left(2 - \frac{S}{S^{**}} - \frac{S^{**}}{S}\right) - \theta R_H^{**} + \left(1 - \frac{R_H}{R_H^{**}}\right)\left(1 - \frac{S^{**}}{S}\right)\right)$$
$$\left(1 - \frac{E_H^{**}}{E_H}\right){}^cD_t^\gamma E_H = \left(1 - \frac{E_H^{**}}{E_H}\right)\left(\omega_{H1}^{**}S - \omega_{H1}^{**}S^{**}\frac{E_H}{E_H^{**}}\right),$$
$$= \omega_{H1}^{**}S^{**}\left(\left(1 - \frac{S\omega_{H1}}{\omega_{H1}^{**}S^{**}}\frac{E_H^{**}}{E_H} - \frac{E_H^{**}}{E_H} + \frac{S\omega_{H1}}{\omega_{H1}^{**}S^{**}}\right)\right),$$
$$\frac{K_1}{\rho}\left(1 - \frac{I_{AH}^{**}}{I_{AH}}\right){}^cD_t^\gamma I_{AH} = \frac{K_2}{\rho}\left(1 - \frac{I_{AH}^{**}}{I_{AH}}\right)\left(\rho E_H - K_2\frac{I_{AH}}{I_{AH}^{**}}I_{AH}^{**}\right),$$
$$= \omega_{H1}^{**}S^{**}\left(\left(1 + \frac{E_H}{E_H^{**}} - \frac{I_{AH}^{**}}{I_{AH}} - \frac{E_H}{E_H^{**}}\frac{I_{AH}^{**}}{I_{AH}}\right)\right),$$
$$\frac{K_2}{\sigma}\left(1 - \frac{I_{CR}^{**}}{I_{CR}}\right){}^cD_t^\gamma I_{AH} = \frac{K_2}{\sigma}\left(1 - \frac{I_{CR}^{**}}{I_{CR}}\right)\left(\frac{I_{AH}}{I_{AH}^{**}} - \frac{I_{cR}}{I_{CR}^{**}}\right),$$
$$= \omega_{H1}^{**}S^{**}\left(\left(1 - \frac{I_{CR}^{**}}{I_{CR}} - \frac{I_{CR}^{**}}{I_{CR}}\frac{I_{AH}}{I_{AH}^{**}} + \frac{I_{AH}}{I_{AH}^{**}}\right)\right),$$
$$\frac{K_2K_3}{\rho\sigma}\left(1 - \frac{T_H^{**}}{T_H}\right){}^cD_t^\gamma T_H = \frac{K_2K_3}{\rho\sigma}\left(1 - \frac{T_H^{**}}{T_H}\right)\left(\frac{I_{AH}}{I_{AH}^{**}} - \frac{I_{cR}}{I_{CR}^{**}} - \frac{T_H}{T_H^{**}}\right),$$
$$= \omega_{H1}^{**}S^{**}\left(\left(1 - \frac{T_H}{T_H^{**}} - \frac{T_H^{**}I_{CR}I_{AH}}{I_{CR}^{**}T_HI_{AH}^{**}} + \frac{I_{CR}I_{AH}}{I_{CR}^{**}I_{AH}^{**}}\right)\right), \quad (26)$$

Hence, Eq. (26) now becomes;

$${}^cD_t^\gamma L(t) \leq \omega_H^{**}S^{**}$$

$$\left(6 - \frac{S^{**}}{S} + \frac{\omega_{H1}}{\omega_{H1}^{**}}\left(1 - \frac{SE_H^{**}}{S^{**}E_H}\right) - \frac{I_{AH}^{**}E_H}{I_{AH}E_H^{**}} - \frac{I_{CR}^{**}I_{AH}}{I_{CR}I_{AH}^{**}}\right) \leq 0.$$

$${}^cD_t^\gamma L(t) \leq \omega_H^{**}S^{**}\beta(R_0^H - 1)\lambda S^{**}$$

Which implies that,

$$\left(6 - \frac{S^{**}}{S} + \frac{\omega_{H1}}{\omega_{H1}^{**}}\left(1 - \frac{SE_H^{**}}{S^{**}E_H}\right) - \frac{I_{AH}^{**}E_H}{I_{AH}E_H^{**}} - \frac{I_{CR}^{**}I_{AH}}{I_{CR}I_{AH}^{**}} - \frac{T_H}{T_H^{**}} - \frac{T_H^{**}I_{AH}I_{CR}}{T_HI_{AH}^{**}I_{CR}^{**}}\right) \leq 0.$$
$$-\beta(R_0^H - 1)\lambda S^{**}\left[K_2S^{**}\left(\frac{S^{**}}{S} - 1 - ln\frac{S^{**}}{S}\right) + \left(\frac{R_H}{R_H^{**}} - 1 - ln\frac{R_H^{**}}{R_H}\right) + \left(\frac{SR_H^{**}}{S^{**}R_H} - 1 - ln\frac{SR_H^{**}}{S^{**}R_H}\right) + \theta R_H^{**}\left(1 - \frac{R_H}{R_H^{**}}\right)\left(\frac{S^{**}}{S}\right)\right]$$

Therefore, ${}^cD_t^\gamma L(t) \leq 0^{**}$ for $R_0^H > 1$. This implies that ${}^cD_t^\gamma L(t) = 0$
${}^cD_t^\gamma L(t) \leq 0$ for $R_0 >.1$. This implies that ${}^cD_t^\gamma L(t) = 0$. If $E_{**} = (S^{**}, E_H^{**}, I_{AH}^{**}, I_{CR}^{**}, T_H^{**}, R_H^{**})$, is the endemic equilibrium point. , then by LaSalle's invariance principle, the endemic equilibrium point is globally asymptotically stable in Ωwhenever $R_0^H > 1$.

Fractional order model numerical results

We employed the generalized fractional Adams-Bashforth–Moulton method described by Chan et al. (2020) to numerically solve the fractional-order Hepatitis C model. The parameters used in the model are listed in Table 1, and simulations were performed for various fractional-order values(γ)**.**

Implementation of fractional Adams–Bashforth–Moulton method

We utilized the method outlined by Baskonus et al., Diethelm& Freed, as detailed in NCDC (2019), Diethelm (1999), Baskonus et al. (2015), and Liu et al. (2023) in our current work. An approximate solution for the fractional Hepatitis C model presented in (6) was obtained using the fractional Adams–Bashforth–Moulton method. The fractional model (6) is now reformulated in Chen et al. (2020) as follows:

$$ {}^{c}D_t^{\gamma} M(t) = N\big(t, m(t)\big), 0 < t < \psi \tag{27}$$

$M^{(n)}(0) = M_0^{(n)}, n = 0,1\ldots, m, m = [\gamma].$

Where $M = (S^*, E_H^*, I_{AH}^*, I_{CR}^*, T_H^*, R_H^*) \in R_+^6$ and $Q\big(t, m(t)\big)$ is a real valued function that is continuous.

Eq. (27) can be therefore be represented using the concept of fractional integral as follows;

$$M(t) = \sum_{n=0}^{m-1} M_0^{(n)} \frac{t^n}{n!} + \frac{1}{\Gamma(\gamma)} \int_0^t (t-\lambda)^{\gamma-1} R\big(y, m(y)\big)\, dy \tag{28}$$

Using the method described in [43], we let the step size $g = \frac{\psi}{N}$, $N \in N$ with a grid that is uniform on $[0, \psi]$ Where $t_c = cr, c = 0,1,1,\ldots N$. Therefore, the fractional order model of Hepatitis C model presented in (6) can be approximated as :

$$S_{k+1}(t) = S_0 + \frac{g^{\gamma}}{\Gamma(\gamma+2)}\left\{\lambda + \theta R_H - \left((\psi_1 I_{AH}^n + \psi_2 I_{CR}^n + \psi_3 T_H^n)\frac{S^n}{N_H^n}\right) - \mu S^n\right\}$$
$$+ \frac{g^{\gamma}}{\Gamma(\gamma+2)} \sum_{y=0}^{k} dy, k+1 \left\{\lambda + \theta R_{Hy} - \left((\psi_1 I_{AHy} + \psi_2 I_{CRy} + \psi_3 T_{Hy})\frac{S_y}{N_{Hy}}\right) - \mu S_y\right\},$$
$$E_{H_{k+1}}(t) = E_{H_0} + \frac{g^{\gamma}}{\Gamma(\gamma+2)}\left\{\left((\psi_1 I_{AH}^n + \psi_2 I_{CR}^n + \psi_3 T_H^n)\frac{S^n}{N_H^n}\right) - K_1 E_H^n\right\}$$
$$+ \frac{g^{\gamma}}{\Gamma(\gamma+2)} \sum_{y=0}^{k} dy, k+1 \left\{(\psi_1 I_{AHy} + \psi_2 I_{CRy} + \psi_3 T_{Hy})\left(\frac{S_y}{N_{Hy}}\right) - K_1 E_{Hy}\right\}, \tag{29}$$
$$I_{AH_{k+1}}(t) = I_{AH_0} + \frac{g^{\gamma}}{\Gamma(\gamma+2)}\{\rho E_H^n - (\alpha_1 + \varphi_1 + \sigma + \delta_1 + \mu) I_{AH}^n\}$$
$$+ \frac{g^{\gamma}}{\Gamma(\gamma+2)} \sum_{y=0}^{k} dy, k+1 \{\rho E_{Hy} - (\alpha_1 + \varphi_1 + \sigma + \delta_1 + \mu) I_{AHy}\},$$
$$I_{CR_{k+1}}(t) = I_{CR_0} + \frac{g^{\gamma}}{\Gamma(\gamma+2)}\{\sigma I_{AH}^n - (\alpha_2 + \varphi_2 + \delta_2 + \mu) I_{CR}^n\}$$
$$+ \frac{g^{\gamma}}{\Gamma(\gamma+2)} \sum_{y=0}^{k} dy, k+1 \{\sigma I_{AHy} - (\alpha_2 + \varphi_2 + \delta_2 + \mu) I_{CRy}\},$$
$$T_{H_{k+1}}(t) = T_{H_0} + \frac{g^{\gamma}}{\Gamma(\gamma+2)}\{\alpha_1 I_{AH}^n + \alpha_2 I_{CR}^n - (\varphi_3 + \delta_3 + \mu) T_H^n\}$$
$$+ \frac{g^{\gamma}}{\Gamma(\gamma+2)} \sum_{y=0}^{k} dy, k+1 \{\alpha_1 I_{AHy} + \alpha_2 I_{CRy} - (\varphi_3 + \delta_3 + \mu) T_{Hy}\},$$
$$T_{H\,k+1}(t) = T_{H0} + \frac{g^{\gamma}}{\Gamma(\gamma+2)}\left\{\alpha_1 I_{AH}^n + \alpha_2 I_{CR}^n - K_4 T_H^n\right\} +$$
$$\frac{g^{\gamma}}{\Gamma(\gamma+2)} \sum_{y=0}^{k} dy, k+1 \left\{\alpha_1 I_{AHy} + \alpha_2 I_{CRy} - K_4 T_{Hy}\right\},$$
$$R_{H_{k+1}}(t) = R_{H_0} + \frac{g^{\gamma}}{\Gamma(\gamma+2)}\{\varphi_1 I_{AH}^n + \varphi_2 I_{CR}^n + \varphi_3 T_H^n - (\theta + \mu) R_H^n.\}$$
$$+ \frac{g^{\gamma}}{\Gamma(\gamma+2)} \sum_{y=0}^{k} dy, k+1 \{\varphi_1 I_{AHy} + \varphi_2 I_{CRy} + \varphi_3 T_{Hy} - (\theta + \mu) R_{Hy}\}.$$

Where

$$S_{K+1}^n(t) = S_0 + \frac{1}{\Gamma(\gamma)} \sum_{y=0}^{k} f_{y,k+1} \left\{\lambda + \theta R_{Hy} - \left((\psi_1 I_{AHy} + \psi_2 I_{CRy} + \psi_3 T_{Hy})\frac{S_y}{N_{Hy}}\right) - \mu S_y\right\},$$
$$E_{HK+1}^n(t) = E_{H_0} + \frac{1}{\Gamma(\gamma)} \sum_{y=0}^{k} f_{y,k+1} \left\{(\psi_1 I_{AHy} + \psi_2 I_{CRy} + \psi_3 T_{Hy})\left(\frac{S_y}{N_{Hy}}\right) - K_1 E_{Hy}\right\},$$
$$I_{AHK+1}^n(t) = I_{AH_0} + \frac{1}{\Gamma(\gamma)} \sum_{y=0}^{k} f_{y,k+1} \{\rho E_{Hy} - K_2 I_{AHy}\}, \tag{30}$$

$$I^{n}_{CRK+1}(t) = I_{CR_0} + \frac{1}{\Gamma(\gamma)}\sum_{y=0}^{k} f_{y,k+1}\left\{\sigma I_{AHy} - K_3 I_{CRy}\right\},$$

$$T^{n}_{HK+1}(t) = T_{H_0} + \frac{1}{\Gamma(\gamma)}\sum_{y=0}^{k} f_{y,k+1}\left\{\alpha_1 I_{AHy} + \alpha_2 I_{CRy} - (\varphi_3 + \delta_3 + \mu)T_{Hy}\right\},$$

$$R^{n}_{HK+1}(t) = R_{H_0} + \frac{1}{\Gamma(\gamma)}\sum_{y=0}^{k} f_{y,k+1}\left\{\varphi_1 I_{AHy} + \varphi_2 I_{CRy} + \varphi_3 T_{Hy} - (\theta + \mu)R_{Hy}\right\}.$$

From (29) and (30) obtained;

$dy, k+1-(k-\gamma)(k+\gamma)^{\gamma}, y=0$

$(k-y+2)^{\gamma+1}(k-\gamma)^{\gamma+1} - 2(k-y+1)^{\gamma+1},\ 1 \le y \le x$

$1, y = k+1$

And

$f_{y,k+1} = \frac{g^{\gamma}}{\gamma}[(k-y+1)^{\gamma}(k-y)^{\gamma}],\ 0 \le y \le k$

Table 1: Values of model parameters used for simulation

Parameter	Description	Value/day	Sources
λ	Recruitment rate of susceptible individuals	0.29	Estimated
θ	The rate at which recovered individuals become susceptible again	0.32	Estimated
μ	The natural death rate for all the compartments .	0.000303	Estimated
ρ	The rate at which individuals become Exposed to acute infection.	0.23	Estimated
α_1	Treatment rate of acute infected individuals.	0.31	Estimated
α_2	Treatment rate of chronic infected individuals.	0.27	Estimated
σ	Progression rate from acute infected I_{AH} to chronic infected I_{CR}	0.31	Estimated
δ_1	The disease induced death rate of infected individuals with acute hepatitis C	0.28	Estimated
δ_2	The disease induced death rate of infected individuals with Chronic hepatitis C	0.31	
δ_3	The disease induced death rate of individuals on treatment but not yet cured,	0.3	Estimated
φ_1	The rate at which acute infected individuals recovered naturally from acute infected I_{AH} to recovered class R_H	0.26	Estimated
φ_2	The rate at which chronic infected I_{CR} individuals recovered naturally from chronic infection I_{CR} to recovered class R_H	0.29	Estimated
φ_3	The rate at which individuals recovered from Hepatitis C due to treatment.	0.25	Estimated
ψ_1	Contact rate of acute infected individuals	0.2	Shen, Xia et al
ψ_2	Contact rate of acute infected individuals	0.26	Shen, Xia et al
ψ_3	Contact rate of individuals on treatment	0.29	Shen, Xia et al

Importance of using the fractional Adam-Bashforth Moulton method in obtaining the numerical solutions of the model

The fractional Adams–Bashforth–Moulton method requires just one extra function evaluation per step while delivering high-order accuracy.

This approach provides automatic error control and is frequently employed in integrated ODE solvers.

It holds potential for applications across diverse fields, including Engineering, Chemistry, and Medicine, and is a valuable tool for numerically solving both partial and fractional-order differential equations.

RESULTS AND DISCUSSION

Numerical Simulation

The graphs from our numerical simulation are shown in this section along with the corresponding interpretations.

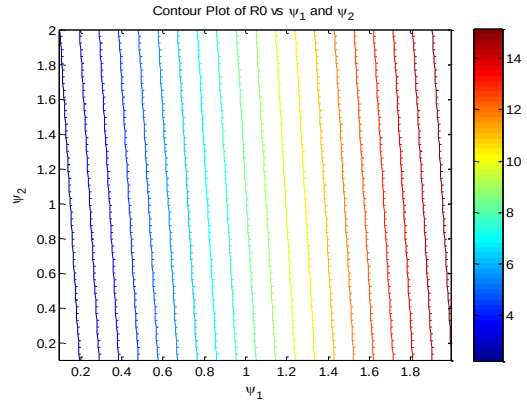

Figure 1(a): Contour plot showing the impact of ψ_1 and ψ_2 on R_0^H

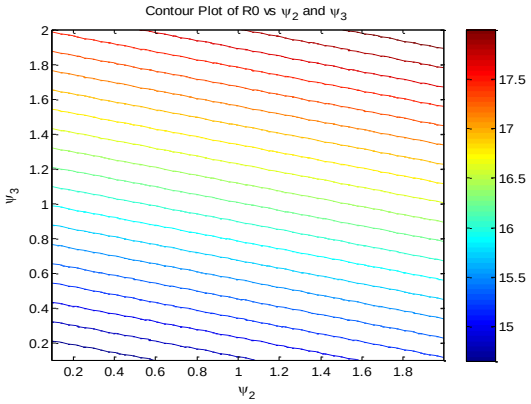

Figure 1(b): Contour plot showing the impact of ψ_1 and $\psi_3 R_0^H$

The graph depicted in Fig. 1(a) illustrates the contour plot of $\psi_1 and \psi_2$ concerning R_0^H. Upon examination of the numerical streams within the graph, it is evident that the maximum value of R_0^H attained by varying these parameters is 0.6, indicating a value below unity (1). This observation suggests that augmenting these parameters would not prompt a significant outbreak of Hepatitis C in the population.Fig. 1(b) illustrates the contour plot of $\psi_1 and \psi_3$ concerning R_0^H . Upon examination of the numerical streams within the graph, it is evident that themaximum value of R_0^H attained by varying these parameters is 0.6, indicating a value below unity (1). This observation suggests that augmenting these parameters would not trigger a significant outbreak of Hepatitis C in the population.

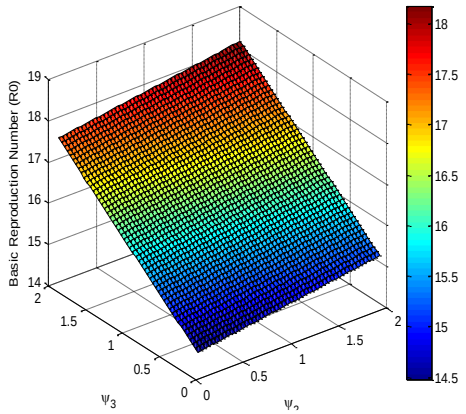

Figure 2(a): Surface plot of R_0^H as a function of $\psi_1 and \psi_2$

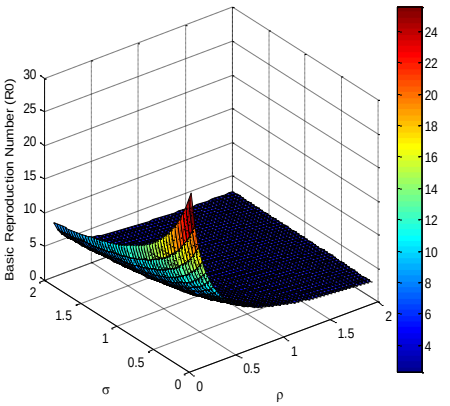

Figure 2(b): Surface plot of R_0^H as a function of σ and ρ

Fig. 2(a), it can be observed that the basic reproduction number R_0^H reaches a peak below one (1) as the values of $\psi_1 and \psi_2$ increase. This indicates that reducing these parameters will ultimately alleviate the impact of Hepatitis C on the population. on the other hand, if appropriate measures are not implemented, $\sigma and \rho$ can exacerbate the prevalence of Hepatitis C. This is evident from their effect on R_0^H , causing it to peak above one (1) as depicted in Fig. 2(b).

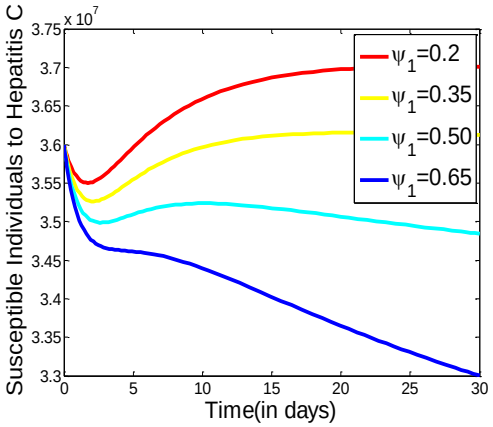

Figure 3(a): Simulation of the susceptible individuals to Hepatitis C

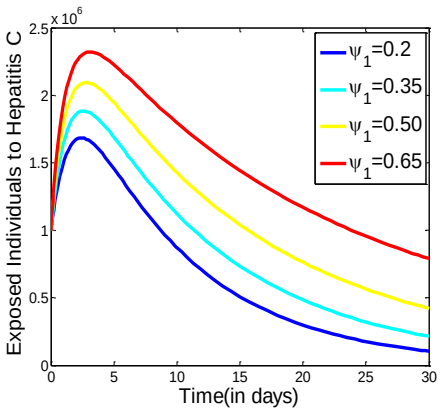

Figure 3(b): Simulation of the exposed individuals to Hepatitis C

Fig (3a) depict the simulation of the effect of the contact rate (ψ_1) of infected individuals with acute hepatitis C on the number of susceptible individuals with Hepatitis C infection. It is observed that, as contact rate (ψ_1) of infected individuals with acute hepatitis C increases, the number of susceptible individuals to hepatitis C disease reduces. Additionally , if we increase the contact rate (ψ_1) of infected individuals with acute hepatitis C to 20%, the number of susceptible individuals to hepatitis C disease reduces will reduce to below 37000000 within 30 days. Fig (3b): depict the simulation of the effect of the contact rate (ψ_1) of infected individuals with acute hepatitis C on the number of Exposed individuals to Hepatitis C infection. It is observed that, as contact rate (ψ_1) of infected individuals with acute hepatitis C increases, the number of Exposed individuals to hepatitis C disease increases. Additionally , if we increase the contact rate (ψ_1) of infected individuals with acute hepatitis C to 20%, the number of Exposed individuals to hepatitis C disease will increase to above 1500000 within 30 days.

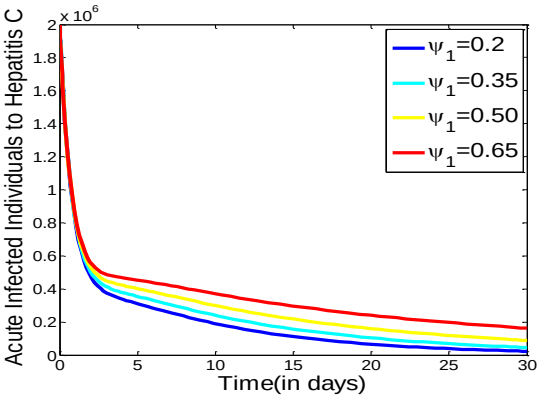

Figure 3(c): Simulation of the acute infected individuals with Hepatitis C

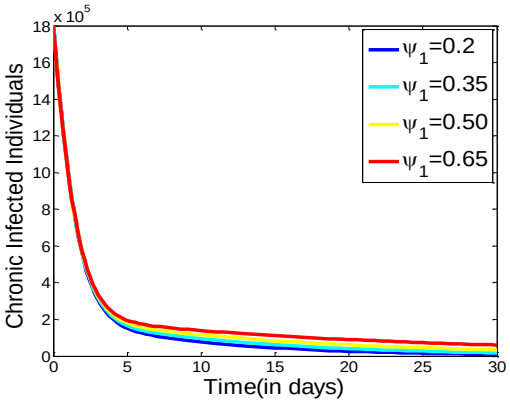

Figure 3(d): Simulation of the chronic infected individuals with Hepatitis C

Fig (3c): depict the simulation of the effect of the contact rate (ψ_1) of infected individuals with acute hepatitis C on the number of infected individuals with acute hepatitis C infection. It is observed that, as contact rate (ψ_1) of infected individuals with acute hepatitis C increases, the number of infected individuals with acute hepatitis C disease increases. Additionally , if we increase the contact rate (ψ_1) of infected individuals with acute hepatitis C to 35%, the number of infected individuals with acute hepatitis C disease will increase to below 200000 with in 30 days.Fig :(3d)depict the simulation of the effect of the contact rate (ψ_1) of infected individuals with acute hepatitis C on the number of infected individuals with chronic hepatitis C infection. It is observed that, as contact rate (ψ_1) of infected individuals with acute hepatitis C increases, the number of infected individuals with chronic hepatitis C disease increases.

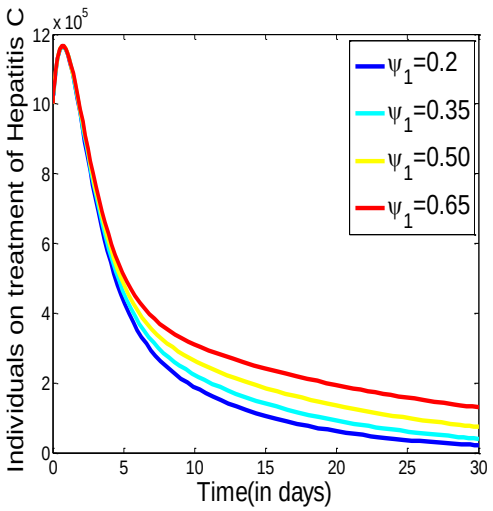

Figure 3(e): Simulation of individuals on treatment of Hepatitis C

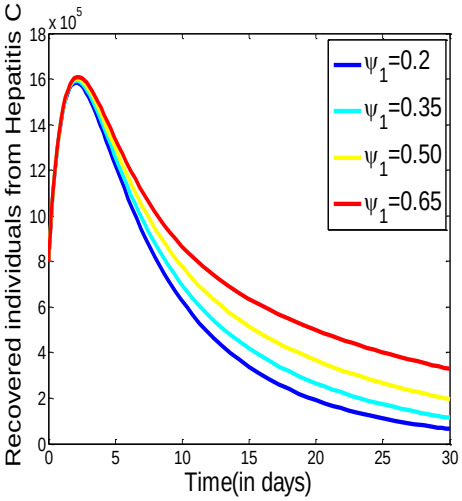

Figure 3(f): Simulation of recovered individuals from Hepatitis C

Fig (3e): depict the simulation of the effect of the contact rate (ψ_1) of infected individuals with acute hepatitis C on the number of individuals on treatment of hepatitis C infection. It is observed that, as contact rate (ψ_1) of infected individuals with acute hepatitis C increases, the number of individuals on treatment of hepatitis C disease will increase. Fig (3f): depict the simulation of the effect of the contact rate (ψ_1) of infected individuals with acute hepatitis C on the number of Recovered individuals from hepatitis C infection. It is practical that, as contact rate (ψ_1) of infected individuals with acute hepatitis C increases, the number of Recovered individuals from hepatitis C disease decreases.

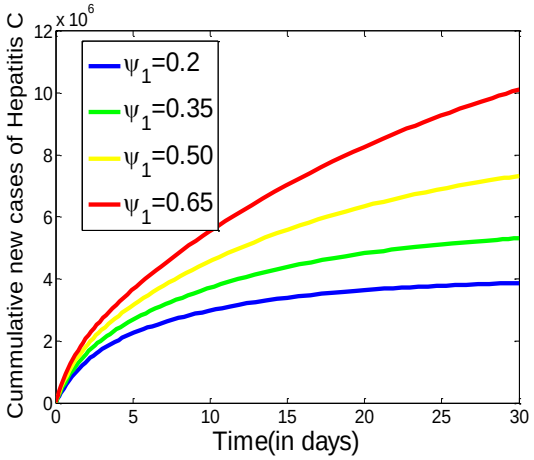

Figure 3(g): Simulation of cumulative new cases of Hepatitis C

Fig (3g) depict the simulation of the effect of the contact rate (ψ_1) of infected individuals with acute hepatitis C on the cumulative new cases of hepatitis C infection. It is observed that, as contact rate (ψ_1) of infected individuals with acute hepatitis C increases, the cumulative new cases of hepatitis C increases. Additionsally , if we increase the contact rate (ψ_1) of infected individuals with acute hepatitis C to 20%, the cumulative new cases of Hepatitis C disease increases to below 4000000 within 30 days.

CONCLUSION

This manuscript presents a mathematical model for the transmission dynamics and control of Hepatitis C using the Caputo fractional derivative. Acknowledging the importance of fractional modeling, we began with a comprehensive theoretical analysis of the fractional Hepatitis C model, focusing on solution existence, uniqueness, and equilibrium stability. We employed the fractional Adams–Bashforth–Moulton method to numerically solve the model. The simulations illustrated the impact of the disease's incidence, taking into account model parameters and various fractional orders of the Caputo operator. Additionally, we conducted simulations by adjusting parameters such as the contact rates between infected and susceptible individuals. The results indicated that enhancing treatment strategies could significantly reduce the prevalence of Hepatitis C in the population. Future work could explore solving non-linear partial differential equations using methods like those presented by Zhang et al. (2022), which offer a general symbolic computing approach for analytic solutions.

REFERENCES

Abdulhamid A, N. Hussaini, Effects of quarantine on transmission dynamics of lassa fever,BayeroJ.PureAppl.Sci.11(2018)397–407.

Acheneje, G.O.,Omale,D., Agbata,B.C., Atokolo,W., Shior,M.M., Bolarinwa,B(2024) Approximate Solution of the Fractional Order Mathematical Model on the Transmission Dynamics on The Co-Infection of COVID-19 and Monkeypox Using the Laplace-Adomian Decomposition Method, International Journal of Mathematics and Statistics Studies, 12(3),17-51

Ahmed I., . Goufo E. F. D,Yusuf A., Kumam .P., Chaipanya P., and Nonlaopon K. (2021), "An epidemic prediction from analysis of a combined HIV-COVID-19 co-infection model via ABC fractional operator," Alexandria Engineering Journal, vol. 60, no. 3, pp. 2979–2995.

Atokolo W a, RemigiusAja .O. ,Omale .D., Ahman .Q. O.,Acheneje G. O., Amos . J. (2024) Fractional mathematical model for the transmission dynamics and control of Lassa fever Journal of journal homepage: www.elsevier. 2773-1863/© 2024com/locate/fraopehttps:// doi.org/10.1016/j.fraope.2024.100110.

Atokolo W a, RemigiusAja .O. ,Omale .D., Paul .R. V.,Amos . J.,Ocha S. O., (2023) Mathematical modeling of the spread of vector borne diseases with influence of vertical transmission and preventive strategies FUDMA Journal of sciences: Vol. 7 No. 6, December (Special Issue), pp 75 -91 DOI: https://doi.org/10.33003/fjs-2023-0706-2174

Atokolo, W., Aja, R. O., Aniaku, S. E., Onah, I. S., &Mbah, G. C. (2022).Approximate solution of the fractional order sterile insect technology model via the Laplace– Adomian Decomposition Method for the spread of Zika virus disease.International Journal of Mathematics and Mathematical Sciences, 2022(1), 2297630.

Baskonus. H.M.,Bulut H., (2015) On the numerical solutions of some fractional ordinary differential equations by fractional Adams Bashforth-Moulton Method, Open Math. 13 1.

Bolarinwa.B, M.M., , (2024) Approximate Solution of the Fractional Order

Bonyah. E., Zarin, R. Fatmawati, Mathematical modeling of Cancer and Hepatitis co-dynamics with non-local and nonsingular kernal, 2020, 2052–2541.https://doi.org/10.28919/ cmbn/5029.

Brawer, F., & Castillo – Chavez, C.(2021). MathematicalModels in Populaiton Biology and Epidemiology. (Vol. 44,Pp: xxiv + 416). New York; Springer.

Chen, S.B. Rajaee F., Yousefpour A., Alcaraz . R. Y., Chu . J.F. Gómez-Aguilar, S. Bekiros, A. Aly,Jahanshahi H.,(2020) Antiretroviral therapy of HIV infection using a novel optimal type-2 fuzzy control strategy, AEJ - Alexandria Eng. J. 60 http://dx.doi.org/10.1016/j.aej.2020.11.009 .

Chen, Y., Wong, K., & Zhao, L. (2023), Modeling the Impact of Vaccination Strategies on Hepatitis C and COVID-19 Coinfection Dynamics, journal of vaccine, vol, 41(15), pages, 2897-2905.

Chikaki, E., Ishikawa, H (2009). A Dengue TransmissionModel in Thailand considering sequential infections with allfour serotypes. J. Infect. Dev. Ctries. 3(9), 711 – 722.

Das, R., Patel, S., & Kumar, A.(2024), Mathematical Modeling of Hepatitis C and COVID-19 Coinfection in Low- and Middle-Income Countries: Challenges and Opportunities, Journal of BMC Public Health, vol, 24(1), pages, 587.

Diethelm .K., (1999) The Frac PECE subroutine for the numerical solution of differential equations of fractional order,.
DOI: https://doi.org/10.33003/fjs-2023-0706-2174 .

Elkaranshawy H. A., Ezzat H. M., and Ibrahim. N. N.,(2020)"Dynamical analysis of a multiscale model of hepatitis C virus infection using a transformed ODEs model,"in 2020 42nd Annual International Conference of the IEEE Engineering in Medicine & Biology Society (EMBC), pp. 2451–2454, Montreal, QC, Canada,.

Garcia, L., Patel, R., & Nguyen, T ,(2022) Dynamic Modeling of Coinfection Transmission: Insights from Hepatitis C and COVID-19, journal of Mathematical Biosciences, vol, 289, pages 112-125.

Liu B. S. Farid, S. Ullah, M. Altanji, R. Nawaz, S.W. Teklu, Mathematical Assessment of Monkeypox disease with the impact of vaccination using a fractional epidemiological modeling approach, Sci. Rep. (2023) http://dx.doi. org/10.1038/541598-023-40745.
Mathematical Model on the Transmission Dynamics on The Co-Infection of

Milici C., G. Draganescu, J.T. Machado, Introduction to Fractional Differential Equations, Springer, 2018.
Nigeria Centre for Disease Control HandBook, Nigeria Centre for Disease Control (NCDC), Viewed February 18 2019 from http://www.ncdc.gov.ng.

Ogabi C.O. ,Olusa T.V.,. Madufor M.A, Controlling lassa fever transmission in Northern part of Edo state Nigeria using SIS model, N. Y. Sci. J. 5 (12) (2012) 190–197.

Ojo M. M.,Goufo. E.F.D. (2022) , Modeling, analyzing and simulating the dynamics of Lassa fever in Nigeria, J Egypt Math Soc 30 (1) http://dx.doi.org/10.1186/s42787-022-00138-x.

Omame,A. M. Abbas, and C. P. Onyenegecha, (2022). "A fractional order model for the co-interaction of COVID-19 and hepatitis B virus,"

Omede B. I, Israel .M.,Mustapha .M. K. , Amos J. ,Atokolo .W. , and Oguntolu .F. A. (2024) Approximate solution to the fractional soil transmitted Helminth infection model using Laplace Adomian Decomposition Method.Journal of mathematics. (2024) Int. J. Mathematics. 07(04), 16-40.

Podlubny .I., (1998) Fractional differential equations, an introduction to fractional derivatives, in: Fractional Differential Equations, to Methods of their Solutions and Some of their Applications, Elsevier,.

Richmond .J.K., Baglole .D.J.,(2003) Lassa fever: epidemiology, clinical features and social consequences, BMJ 327 1271–1275.

Smith, J., Johnson, A. B., & Lee, C.(2023) Modeling the Coinfection Dynamics of Hepatitis C and COVID-19: A Systematic Review" journal of Epidemiology and Infection, vol, 151(7), pages , 1350-1365.

Ullah. A.Z. T. Abdeljawad, Z. Hammouch, K. Shah, A hybrid method for solving fuzzy Volterra integral equations of separable type kernels, J. King Saud Univ. - Sci. 33 (2020) http://dx.doi.org/10.1016/j.jksus.2020.101246.

VandenDriessche .Watmough P., J.,(2002) , Reproduction numbers and Sub-threshold endemic equilibria for compartmental models of disease transmission, Math. Biosci. 180 (1–2) 29–48.

Wang, X., Kim, S., & Gupta, M. (2024) Modeling of Hepatitis C and COVID-19 Coinfection Hotspots: A Geospatial Analysis Journal of Geospatial Health, vol, 16(2), pages, 87-99.

Wong, T., Patel, M., & Lee, E.(2024) Mathematical Modeling of Coinfection Transmission in the Context of Vaccination Strategies: Hepatitis C and COVID-19, Journal of Theoretical Biology, vol, 512, pages, 110367

Yunus A.O, M.O. Olayiwola, M.A. Omolaye, A.O. Oladapo, A fractional order model of lassa fever disease using the Laplace-Adomian decomposition method, Health Care Anal. 3 (2023) 100167, www.elsevier.com/locate/health.Health care Analytics.

Yunus, A. O., Olayiwola, M. O., Adedokun, K. A., Adedeji, J. A., &Alaje, I. A. (2022). Mathematical analysis of fractional-order Caputo's derivative of coronavirus disease model via Laplace Adomian decomposition method.Beni-Suef University Journal of Basic and Applied Sciences, 11(1), 144.

Z. Ali, A. Zada, K. Shah, Existence and stability analysis of three point boundary value problem, Int. J. Appl. Comput. Math.3 (2017) 651–664, http://dx.doi. org/10.1007/s40819-017-0375-8.

Zhang .R.F., M.-C.Li, J.Y. Gan, Q. Li, Z.-Z.Lan, (2022). Novel trial functions and rogue waves of generalized breaking soliton equation via bilinear neural network method, Chaos Solitons Fractals 154 (C) . Results in Physics, vol. 37, article 105498.